Article

The influence of lateral spacing of TiO_2 nanotube coated surfaces on the early in vivo osseointegration

Andreea Mariana Negrescu , Iuliana Ionascu , Madalina Georgiana Necula , Niculae Tudor , Maksim Kamaleev , Otilia Zarnescu , Anca Mazare * , Patrik Schmuki , Anisoara Cimpean *

Posted Date: 26 November 2024

doi: 10.20944/preprints202411.1944.v1

Keywords: nanotopographic surfaces; TiO_2 nanotubes; intertube spacing; osteoblasts; in vivo osteointegration

Article

The influence of lateral spacing of TiO_2 nanotube coated surfaces on the early in vivo osseointegration

Andreea Mariana Negrescu [1,2£], Iuliana Ionascu [3£], Madalina Georgiana Necula [1], Niculae Tudor [3], Maksim Kamaleev [4], Otilia Zarnescu [1], Anca Mazare [5*], Patrik Schmuki [5,6] and Anisoara Cimpean [1*]

[1] Department of Biochemistry and Molecular Biology, Faculty of Biology, University of Bucharest, 91-95 Spl. Independentei, 050657 Bucharest, Romania; andreea-mariana.negrescu@bio.unibuc.ro; necula.madalina92@gmail.com; otilia.zarnescu@bio.unibuc.ro; anisoara.cimpean@bio.unibuc.ro;
[2] Research Institute of the University of Bucharest (ICUB), University of Bucharest, 050657 Bucharest, Romania;
[3] Faculty of Veterinary Medicine, University of Agronomic Sciences and Veterinary Medicine, 105 Spl. Independentei, 050097 Bucharest, Romania; iuliana.ionascu@usamv.ro; niculae.tudor@fmvb.usamv.ro;
[4] Department of Materials Science and Engineering, Chair of General Materials Properties, Friedrich-Alexander-University of Erlangen-Nürnberg, Martensstraße 5, 91058 Erlangen, Germany; maksim.kamaleev@fau.de
[5] Department of Materials Science and Engineering, WW4-LKO, Friedrich-Alexander-University of Erlangen-Nürnberg, Martensstrasse 7, 91058 Erlangen, Germany; anca.mazare@fau.de; schmuki@ww.uni-erlangen.de;
[6] Regional Centre of Advanced Technologies and Materials, Šlechtitelů 27, 78371 Olomouc, Czech Republic;
* Correspondence: A.C. anisoara.cimpean@bio.unibuc.ro; A.M. anca.mazare@fau.de
[£] Contributed equally and share first authorship

Abstract: Due to the bio-inert nature of titanium (Ti) and subsequent accompanying chronic inflammatory response, the implant's stability and function can be significantly affected, leading in time to a poor osseointegration process. To overcome this challenge and improve the overall performance of Ti implants, various surface modifications have been employed, amongst them the deposition of titanium oxide (TiO_2) nanotubes (TNTs) onto the native surface through the anodic oxidation method. While numerous in vitro and in vivo studies have already reported the importance of nanotube diameter on cell behaviour and osteogenesis, information regarding the effects of nanotube lateral spacing on the *in vivo* osseointegration process is insufficient and hard to find. Considering this, in the present study two types of TNTs with different lateral spacing, e.g. 25 nm (TNTs) and 92 nm (spTNTs) were fabricated and comparatively investigated in terms of their effect on the early peri-implant new bone formation. The microscopic examination at 1-month post-implantation revealed that both nanotubular surfaces, particularly spTNTs, were capable of inducing new bone formation without a significant bone destruction. Overall, our results indicate that the lateral spacing of the TNT-coated Ti surfaces can influence the *in vivo* outcome, thus representing a significant factor in implant design.

Keywords: nanotopographic surfaces; TiO_2 nanotubes; intertube spacing; osteoblasts; in vivo osteointegration

1. Introduction

With the unprecedented aging of the world's population, the need for medical implantable devices suitable for oral rehabilitation and orthopedic-related traumas/diseases is predicted to grow in accordance with their high demand [1]. With a favourable combination of properties such as a high mechanical strength approximating bone, chemical stability, good biocompatibility and low costs, titanium (Ti) and its alloys continue to be the first-choice type of material in diverse clinical applications for hard tissue replacements [2]. However, in spite of the advantageous properties, the bio-inert nature of the untreated Ti-based biomaterials can compromise the initial cell adhesion and the subsequent osseointegration process, and can be a main reason why implant failure can sometimes occur [3]. By modifying the biomaterial's surface, the long term-performance of the

 doi:10.20944/preprints202411.1944.v1

implant can be greatly improved through the enhancement of the structural and functional connections established between the native bone tissue and the implant's surface [4]. In addition, through surface modification, the implantable biomaterial can also be endowed with improved properties such as better wear and corrosion resistance, favourable biocompatibility and appropriate surface wettability [5].

In the last decade, the nanotopographically altered biomaterials, especially those within the dimensional range of 100 nm, have received special attention due to their superior properties such as an increased biological response and a larger surface area [6]. Amongst the various methods used for their synthesis, the electrochemical anodization technique has been recognised as one of the most reliable strategies in the generation of nanophase topographies (e.g., TiO_2 nanotubes) on Ti-based biomaterials in a simple, inexpensive and reproducible way [7]. In addition, this versatile technique allows the formation of highly ordered nanotube features of controlled nano-scale dimensions for an effective biological performance [5]. TiO_2 nanotubes (TNT) synthesised via the electrochemical anodization technique have been the main point of focus in numerous *in vitro* studies, mainly due to their outstanding characteristics, such as an excellent biocompatibility, mechanical rigidity, pore controllability, evenness of pore distribution, high surface area, high loading capability and chemical stability [8], properties which proved to favour bone cell adhesion, proliferation and differentiation [3, 9]. Moreover, it was also established that the textured Ti surfaces can provide larger bone implant contact areas and an improved bone bonding strength in comparison to smoother surfaces, leading to a more favourable in vivo osseointegration process [10]. E.g., Bjusten et al. [10] investigated the in vivo bone bonding strength of two different nanotubular Ti surfaces, namely TiO_2 nanotubes and TiO_2 grit-blasted surfaces, and the reported results indicated that after four weeks of implantation in rabbit tibias, the nanotubular surface was capable of improving the bone bonding strength by as much as nine-fold when compared to the Ti grit-blasted implant. Likewise, the histological analysis revealed a larger bone-implant contact area and an improved new bone formation on the TiO_2-nanotube modified surface. In another in vivo study, von Wilmowsky et al. [11] examined by comparison the osteogenic potential of a TiO_2 nanostructured implant possessing individual tube diameter of 30 nm with that of an untreated standard Ti surface. The immunohistochemistry analysis revealed a higher collagen type-1 expression starting from day 7 up until day 30 for the nanostructured implants in comparison to the control group, suggesting that these implants could influence new bone formation by enhancing the osteoblast function in the early stage of bone development. Similar results were also obtained by Kang et al. [12], where in their study the osseointegration potential of several surface-treated TiO2 nanotubular implants with various diameters (30 nm, 70 nm and 100 nm) was compared to that of an untreated flat Ti surface. Overall, the results proved the superiority of the TiO_2 nanotubular surfaces in regards to the osseointegration process when compared to the untreated surface, but when analysed from a time point of view, it became clear that between the three modified surfaces, only the 30 nm- and 70 nm-diameter TiO2 nanotubes were capable of improving new bone formation and implant osseointegration. Moreover, in another study, the effects of TiO_2 nanotubes with the same diameters of 30 nm, 70 nm and 100 nm on the in vivo osseointegration process were investigated by studying the gene expression and new bone formation in the vicinity of the implants. Compared to the machined Ti implant, the TiO_2 nanostructured surfaces, especially with a nanotube diameter of 70 nm, led to a significant increase in bone-implant contact area and gene expression levels [13]. Furthermore, the beneficial effects of the 70 nm nanotube diameter were also confirmed by Jang et al. [14], where miniscrews coated with 70 nm diameter TiO2 nanotubes were implanted in the legs of New Zealand white rabbits for 8 weeks. The histological analysis revealed that the miniscrews with the modified surface showed not only a greater mean bone-implant contact area (52.8%) than the control (29.3%) but also a mean bone volume ratio with an 81% increase. As observed, while the knowledge regarding the influence of nanotube diameter on the osteoblast behaviour is quite extensive, with numerous in vitro [15-19] and in vivo studies [10-14, 20-21], little effort has been made in trying to understand how other topographical characteristics, such as titania nanotube lateral spacing, can influence the response of the bone-derived cells. In a previous in vitro study, our team demonstrated that the TNTs intertube spacing

 doi:10.20944/preprints202411.1944.v1

can influence the osteoblasts in vitro behaviour, leading to a more pronounced osteogenic activity of the MC3T3-E1 cells grown on surface of the TiO_2 nanotubes with a larger intertube spacing (80 nm) in comparison with closed-packed nanotubes (intertube spacing of 18 nm) [9]. However, to fully prove the enhancing effect of intertube spacing on the early osseointegration process, an in vivo study which involves the direct contact between native bone tissue and the newly designed implant surfaces is necessary. Considering this, the aim of the present study was to investigate the effects of the TiO_2 nanotubes with an intertube spacing of 25 nm (TNTs) and 92 nm (spTNTs) on the early in vivo implant osteointegration process.

2. Materials and Methods

2.1. Implant preparation and characterization

For control and additional material characterization, the tubes on foils were also obtained, following the previously established anodization conditions [9, 22]. Briefly, for closed-packed nanotubes Glycerol (>99.7% p.a. Roth, Karlsruhe, Germany):H_2O (70:30 vol.%) + 0.5 wt.% NH_4F (>98% p.a. Roth, Karlsruhe, Germany) at 21V for 2h, and spaced nanotubes in Diethylene glycol (>99.5% p.a. Roth, Karlsruhe, Germany) + 4 wt.% HF (HF 40%, Sigma Aldrich, Germany) + 0.3 wt.% NH_4F + 7 wt.% H_2O, at 27 V, 4h at 30°C.

The in vivo animal studies were performed with Ti-based pins with a diameter of 1 mm and a length of 16 mm. The Ti pins were cut from Ti wire (Ti 99.6% purity) initially with a 2.2 cm length for use in the anodization process. The implants were ultrasonicated in acetone, ethanol for 5 min each, followed by rinsing with distilled water and drying in a nitrogen stream. The Ti pins were chemically etched for 2 min in a chemical etching solution consisting of 5M HNO_3 and 40 g/L HF. After etching, the pins were rinsed with distilled water and dried in a nitrogen stream, and used as the working electrode in the electrochemical anodization. Compared to nanotube layers grown on Ti foil, for the Ti pins, the anodization conditions were optimized. Anodization was performed in a beaker, using two Pt electrodes as the cathode and Ti pins as an anode. The anode consisted of four Ti pins (2.2 cm) welded on a Ti wire, and the distance of the anode to the corresponding Pt electrode was of 2 cm. The closed-packed nanotubes were obtained by anodizing the Ti pins in an electrolyte containing Glycerol:H_2O (70:30 vol.%) + 0.5 wt.% NH_4F, at 19.5 V, for 1 h 45 min, at room temperature, using 45 mL electrolyte. The spaced nanotubes were obtained in an electrolyte containing Diethylene glycol + 2 wt.% HF (HF 40%) + 0.3 wt.% NH_4F + 1 wt.% H_2O, at 77 V for 4 h, using 115 mL of electrolyte. After anodization, the nanotubes were washed with water and dried in a nitrogen stream, except for the spaced nanotubes, which were in addition first immersed in ethanol for 20 min.

The morphology of the nanotubular layers in terms of tube diameter, spacing, and tube length was evaluated by means of scanning electron microscope (SEM, FE-SEM 4800SEM, Hitachi, Japan). The chemical composition was evaluated by X-ray photoelectron spectroscopy (XPS, PHI 5600, US) by sputtering with Ar+ sputtering (3 nm/ min calibrated to Si/SiO_2).

These nanotube layers were used for further characterization, including, SEM, atomic force microscopy (AFM), and nanoindentation measurements. AFM measurements were performed on Agilent LS5600 (cantilevers SSS-SEIHR -10) in tapping mode. Nanoindentation measurements were performed with a Nanoindenter XP (Keysight, USA), using a diamond Berkovich tip (Synton MDP, Switzerland) coupled with the Continuous Stiffness Measurement (CSM) option and 450 nm depth indents. At least eight indents from each morphology (including the two nanostructured layers, and the bare Ti) were used for evaluating the hardness and elastic modulus.

2.2. Animals

In the current study, a total of 8 heathy adult male Wistar rats with a body weight of 0.25 kg, were randomly divided into two experimental groups (4 animals per group), according to the type of implant surface used and experimental time period. Prior to the surgical procedure, the animals were kept in acclimatized cages for 2 weeks, where their food and water intake were carefully monitored. All of the animal experiments were approved by the Bioethics Committee of the

 doi:10.20944/preprints202411.1944.v1

University of Agronomic Sciences and Veterinary Medicine of Bucharest (Approval code No. 07/28.06.2016) and were conducted according to the international, national and institutional guidelines for the care and use of animals.

2.3. Surgical procedure and post-operative care

To achieve the anaesthetic state necessary for the surgical procedure, the animals have been submitted to the intraperitoneal administration of an anaesthetic mixture containing 100 mg/mL ketamine (1.2 mL) and 0.5 mg/mL dexdomitor (0.8 mL) in 2 mL of saline solution. Moreover, the sustained anaesthetic state was accomplished by mask inhalation of isoflurane vaporised at concentrations of 1-1.5 vol.%. Once the animals have been put under general anaesthesia and the surgical area was shaved and disinfected, a 3 cm longitudinal incision on the external side of the thigh was made in order to cut open the skin and dissect the muscle tissue found beneath (**Figure 1a**). Afterwards, using a Dental Unit cutter, a 2 cm - long, linear, longitudinal fracture was created transversally in the middle third of the femur's diaphysis (**Figure 1b-c**) and the implant was inserted intramedullary (in both posterior legs) through the newly generated fracture (**Figure 1d**). In the end, the thigh muscle was sutured with absorbable polydioxanone (PDS 3/0) threads in separate points, whereas the skin above was sutured with nylon (4/0) threads in a simple continuous pattern. To confirm the position of the implants, an X-ray analysis of the areas subjected to surgery was performed immediately after this intervention (**Figure 2**). With regards to the post-operative care, the animals were given antibiotics (Enrofloxacin – 10 mg/kg BW) and anti-inflammatory drugs (Meloxicam – 0.2 mg/kg BW) daily, for a period of 6 days. Furthermore, no morbidity or mortality was recorded during 6 and 30 days of the experimental period and the surgical incision was left to heal naturally without any medical intervention.

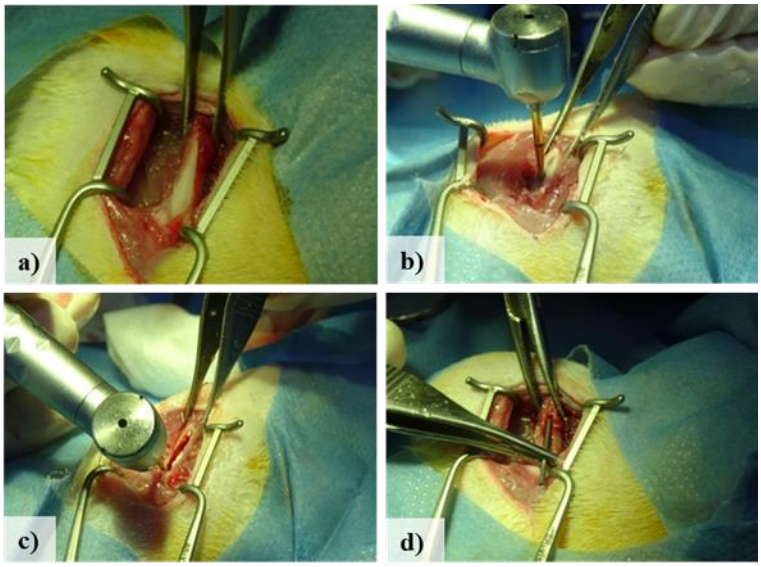

Figure 1. Representative photographs showing the bone implant surgical procedure: **a)** longitudinal incision on the outer side of the thigh to cut the skin and dissect the underlying muscle tissue; **b-c)** longitudinal fracture transverse to the middle third of the femoral diaphysis; **d)** implant insertion.

 doi:10.20944/preprints202411.1944.v1

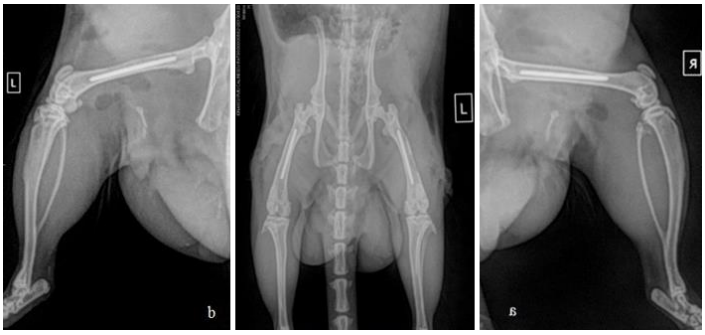

Figure 2. The X-ray analysis of the areas subjected to surgery immediately after the medical intervention.

2.4. Post-operative tissue harvesting

At 6 and 30 days post-implantation, the animals were subjected to the same premedication as in ***Section 2.3*** in order to achieve the anaesthetic state necessary for the surgical removal of the bone specimens. Following anaesthesia, the skin was sectioned on the external side of the thigh, in a longitudinal incision of 3 cm, which allowed the removal of the bilateral femurs, together with the surrounding tissue, by disarticulation. In the end, the animals were euthanized by intraperitoneal administration of 0.5 ml of T61.

2.5. Histological examination

Immediately after euthanasia, the harvested bone samples were firstly fixed for 72 h in a 4% buffered formaldehyde solution, decalcified for 8 days in 5% nitric acid solution, washed for 24 h in 5% solution of sodium sulphate and only when the bone structures became soft, the specimens were embedded in paraffin wax. Sections of 8 μm in thickness were obtained using a rotary microtome (MICROS Produktions-und HandelsgesmbH) and for the histological examination, the Alcian Blue (pH 2.5) and haematoxylin and eosin (HE) staining methods were employed. The photomicrographs were taken by digital camera (AxioCam MRc 5; Zeiss) driven by software AxioVision 4.6 (Zeiss). Moreover, in order to assess the thickness of the newly formed bone tissue, the distance between the outer and the inner surfaces of the bone tissue was measured using the Axio-Vision software, Version 4.6 (Carl Zeiss). The wall thickness was measured at 6 random points and the mean thickness of each newly formed bone tissue was compared.

3. Results

3.1. TiO_2 nanotubes

In the present work, we tailored two different types of anodic TiO_2 nanotubes, the typical close-packed nanotubes, or TNTs (such layers have only some minor spacing at the tube top), and spaced nanotubes denoted as spTNTs, which show a distinct tube-to-tube spacing which is also directly proportional to the nanotube diameter, as schematically shown in **Figure 3a-f**. Such nanotubes are typically grown in fluoride-containing organic electrolytes based on diethylene glycol, dimethyl sulfoxide etc. [9, 23-28], and the corresponding nanotube layers grown on Ti foil are evaluated in **Figure 3**.

From the SEM images in **Figure 3a-d,** the nanostructures have similar morphology, except for the spacing in between nanotubes which is varied. The obtained classical TNTs have an average tube diameter of 79.4 nm (±14.2 nm) and a tube spacing at the tube tops of 22.4 nm (± 5.9 nm). In contrast, the spTNTs have a tube diameter in a similar range (83.1 nm ±17.1 nm) and a spacing of 83.5 nm (± 11.6 nm). Both nanotube layers have an average tube length of 0.8 μm. The chemical composition of such tubes is similar to previously obtained morphologies [9, 22], and consists of C, O, Ti and F; the at.% compositions shown in the sputter-depth profiles (first 60 nm of the layers - **Figure 3i**) confirm the TiO_2 nature of the oxide with ≈6.5 at.% F and ≈11.5 at.% F for the TNTs and spTNTs, respectively.

 doi:10.20944/preprints202411.1944.v1

Following, the surface roughness and topography of the layers was evaluated from AFM (**Figure 3g-h**). The 3D AFM images clearly show the topographical differences between the two nanostructures (with a root mean-square roughness, Rq, of 42.06 nm and 119.9 nm, respectively). Corresponding line profiles (average of three individual profiles) show that the TNTs have a height of up to 0.3 μm for the TNTs and almost 0.6 μm for the spTNTs.

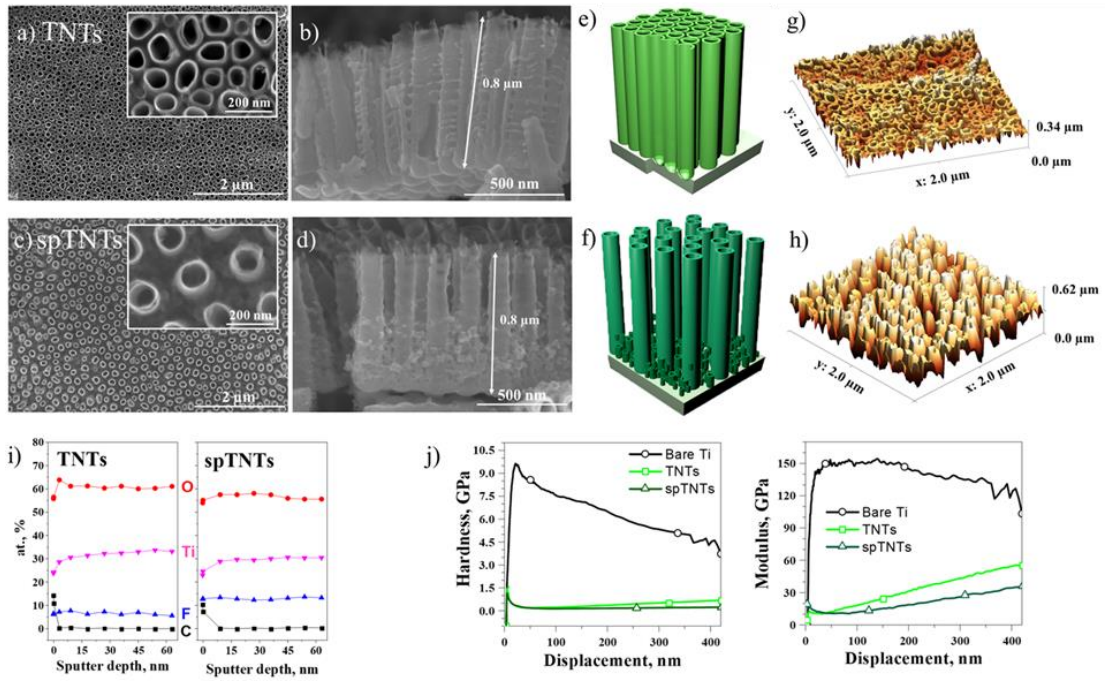

Figure 3. Anodic TiO_2 nanotubes obtained on Ti metal foil: a-d) SEM images of the anodic layers for a,b) TNTs and c,d) spTNTs, including cross-section SEM image; e-f) corresponding 3D schematic of TNTs and spTNTs, respectively; g,h) corresponding 3D AFM images for the TNTs and spTNTs. i) XPS sputter depth profiles showing the at.% composition in the first 60 nm of the layers. j) Nanoindentation measurements for bare Ti (control) and the two different nanotube layers, with hardness (left panel) and elastic modulus (right panel).

Especially for biomedical implants, the nanostructured layers have to be mechanically durable, therefore we performed nanoindentation measurements on both bare Ti and the investigated layers (**Figure 3j** for the hardness and elastic modulus). As shown in **Figure 3j** (left panel), the bare Ti sample shows a hardness of ≈4.5-8.5 GPa. While for the nanotube layers, if we consider the values up to 80nm displacement (which is less than 10% of the total height of the nanotubes, and so no influence from the substrate) [29], this leads to ≈0.5-1.0 GPa. The elastic modulus of Ti is ≈120-150 GPa, while for the nanotube layers (similarly at 80nm displacement) the elastic modulus is ≈10-20 GPa. The observed decreases can be attributed to nanostructure formation, and with increasing displacement the influence of the substrate can be observed.

Following, similar morphology nanotube layers were grown on Ti pins with diameters of 1mm (see also as shown schematically in **Figure 4**), and for this reason, the anodization conditions were optimized and more so for the spTNTs – for the detailed optimized conditions, please see the experimental section. **Figure 4 (a,b)** shows the tube morphology of the layers grown on pins, with tube layers with 1.0μm thickness. The average diameter of the layers is ≈82 - 92 nm, namely 83 nm ± 17 nm for the TNTs and 91 nm ± 19 nm spTNTs, but with different spacing of 25 nm ± 4 nm for TNTs and 92 nm ± 25 nm for spTNTs. An overview of feature size (diameter, spacing) as a function of the used substate (foil or pin) is listed in **Figure 4c**.

 doi:10.20944/preprints202411.1944.v1

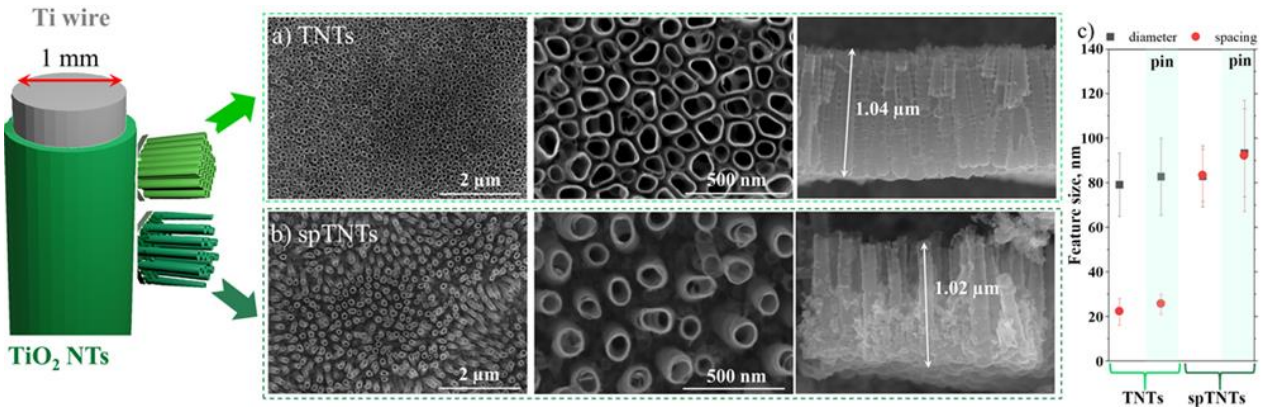

Figure 4. Anodic TiO_2 nanotubes obtained on Ti pins for in-vivo tests: schematic representation and corresponding SEM images of the anodic layers for a) TNTs and b) spTNTs. The SEM images include lower magnification to show the layer uniformity, higher magnification to observe the tube morphology and cross-section images for the lengths of the nanotubes. c) Feature size (diameter, spacing) of the designed TNTs and spTNTs, depending on the substrate (foil or pin).

3.2. The histological appearance of the post-implant tissue

Since the histological characterization of the osseointegration process is crucial for a more in-depth understanding of the intimate relationship established between the damaged bone tissue, the implant and the ability of the material to support new bone formation, the short- and long-term in vivo evaluation of the biological behaviour of two nanostructured Ti-based implants (TNTs and spTNTs) was assessed through the histological analysis of bone sections harvested from the animal subjects at 6 and 30 days post-implantation.

The histological analysis of the peri-implant tissue harvested at 6 days post-implantation showed visible dissimilarities between the investigated biomaterials, as seen in **Figure 5**. Thus, the bone sections from the animal subjects with the modified Ti-based implants highlighted the existence of a thin fibrous tissue adjacent to the peri-implant site in case of both implants. However, the adjacent bone marrow presented a different aspect depending on the features of the nanotubular TiO_2 structures generated on the surface of the Ti-based implant, i.e., with the spTNTs pin leading to a slight modification in the bone marrow structure (**Figure 5b**), as opposed to the TNTs-coated implant, where the structure and cellularity of the bone marrow did not appear to suffer any alterations (**Figure 5a**). It is important to mention, that regardless of bone marrow alteration, in case of both modified surfaces, the ability of the osteoprogenitor cells to differentiate and that of the osteoblasts to secrete osteoid was not affected, as evinced by the presence of the osteoid-secreted osteoblasts.

 doi:10.20944/preprints202411.1944.v1

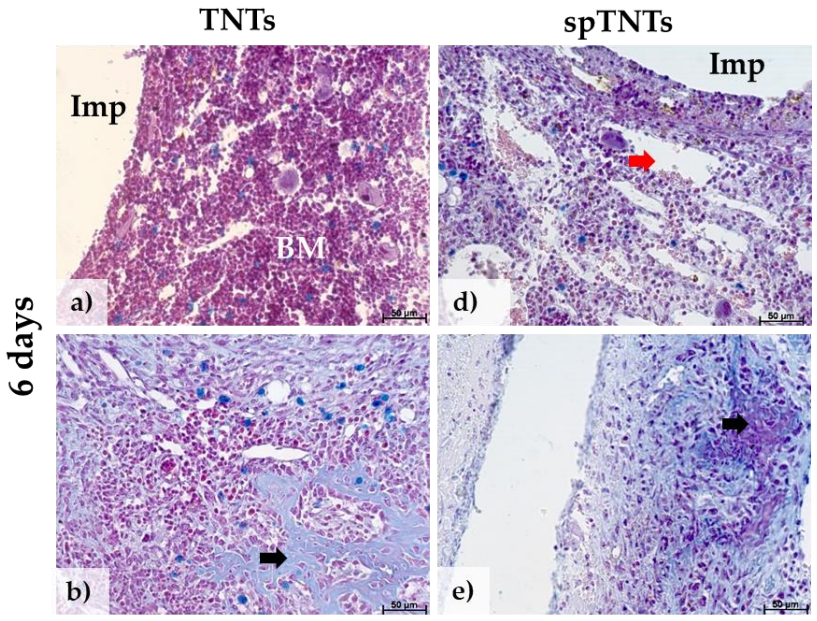

Figure 5. Hematoxylin-eosin (HE) staining of bone sections surrounding the Ti-based implants: a-b) TNTs and d-e) spTNTs, harvested 6 days after the surgical intervention. BM, bone marrow; Imp, intra-medullary implant site. Red arrow – altered bone stroma; black arrows – unmineralised bone tissue (osteoid) secreted by osteoblasts. Scale bar: 50 μm.

In contrast with the results observed at 6 days post-implantation, the histological analysis of the bone sections harvested at 30 days post-implantation highlighted a progressive new bone formation. Thus, **Figure 6** reveals the presence of a noticeable compact adherent newly formed bone tissue (NTB) with no evidence of fibrous tissue formation for both Ti-based implants. In addition, the histological measurements of the newly formed bone tissue (**Table 1**) revealed that the mean thickness of the mineralised tissue in the case of spTNTs implant was higher than the TNTs implant, however with no significant differences between the two analysed TNT-based implants (**Figure 7**). These results suggest that the spTNTs implant can provide a favourable microenvironment for the osteoblasts to promote the ingrowth of mineralised tissue for an enhanced osseointegration process. Moreover, it is noteworthy that no foreign body reaction was observed in either of the implanted animals, indicating that the implants are well tolerated.

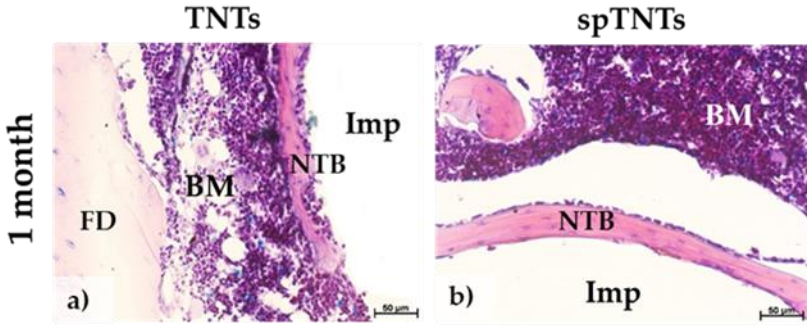

Figure 6. Hematoxylin-eosin (HE) staining of bone tissue surrounding the implants: a) TNTs and b) spTNTs, at 30 days post-implantation. Imp, intra-medullary implant site; BM, bone marrow; FD, femoral diaphysis; NTB, newly formed trabecular bone. Scale bar: 50 μm.

 doi:10.20944/preprints202411.1944.v1

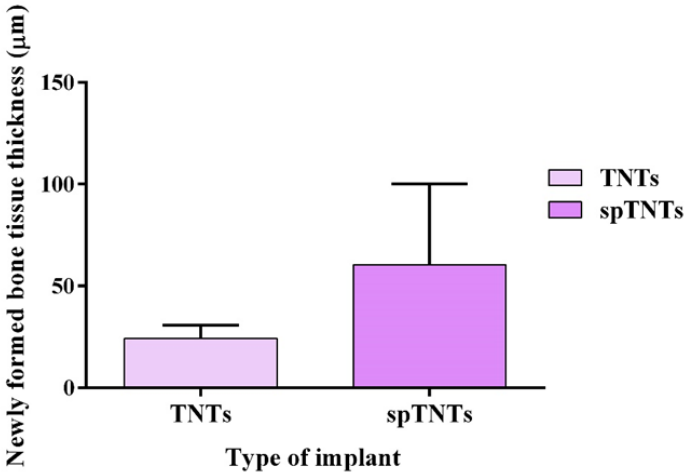

Figure 7. Comparison of newly formed bone tissue thickness (µm) on the transverse histological section of bone (means ± SD) in case of TNTs (24.37±6.5), and spTNTs implants (60.44±39.70).

Table 1. The thickness of the newly formed bone tissue around the analysed nanotubular Ti-based implants after 30 days of implantation.

Type of implant	Newly formed bone tissue thickness (µm)
TNTs	18.08
spTNTS	32.19

One of the most important aspects of bone-implant integration is represented by the enhancement of the functional activity of osteoblasts at the peri-implant interface without any fibrotic tissue formation [30]. However, the majority of modern orthopedic implantable devices present a reduced lifespan due to the establishment of an inappropriate cell–material initial interaction, an event with a key role in the wound healing process, which is heavily dependent on the specific surface properties of the material (e.g. wettability, roughness, topography, etc.) [31].

As evinced by data reported in literature, by modifying the Ti-based implant's surface through anodic oxidation (formation of titania nanotubes), an enhanced new bone formation and osseointegration was observed. For example, Alves-Rezende et al. [32] demonstrated that as opposed to a pure Ti implant, the nanostructured TiO_2 surface led to an improved wettability, an increased osteoblastic cells' migration and implicitly, an enhanced bone-to-implant contact (BIC). Similar, Wang et al. [33] reported that hydrogenated superhydrophilic TiO_2 surfaces were able to significantly accelerate the new bone formation and osseointegration processes, both in the early and later stages. In addition, in another study by Tao et al. [1], the in vivo investigations revealed that between the three newly proposed TNTs surfaces with different nanotube diameter (e.g. 30 nm, 70 nm and 110 nm), the TNT-70 implant exhibited the highest potential to improve new bone formation and BIC, as evinced by the more mature and thicker new bone tissue observed at the peri-implant site. Furthermore, apart from the advantageous surface characteristics, the anodic TiO_2 nanotubes can also be used as drug delivery platforms for various bioactive elements, molecules and compounds capable of promoting bone cell differentiation and new tissue formation [34]. By modifying the surface of a Ti screw with silicon (Si) doped TiO_2 nanotubes, the histological analysis revealed an improved new bone formation and a superior bone-implant bonding strength [35]. In another study, a gallium oxide (Ga_2O_3) coated TNT drug delivery platform was designed based on the hypothesis that the release of Ga^{3+} ions in a sustainable manner could enhance the osteogenic ability of the Ti-based implant. The in vivo analysis demonstrated that the newly fabricated construct was capable of promoting new bone formation through an enhancement in the osteogenesis-related gene expression [36]. Similarly, the incorporation of platinum (Pt) [37] and strontium (Sr) [38] into TNTs facilitated an efficient mineralization and led to the creation of surfaces with a higher interfacial bonding strength.

 doi:10.20944/preprints202411.1944.v1

Starting from the hypothesis that the lateral spacing of the TiO_2 nanotubes can contribute to the continuous flow of the cell culture medium in an in vitro microenvironment, as well as the exchange of gases, nutrients and signalling molecules, thus stimulating the cellular metabolism and better mimicking the in vivo conditions [19, 39], in an initial in vitro study our team investigated the effect of titania nanotube spacing on the MC3T3-E1 pre-osteoblast cell function with interesting results. Thus, depending on the type of nanostructure, the data obtained revealed different cellular responses in terms of cytomorphology, actin cytoskeleton organization, cell spreading area and pattern of focal adhesions, while the osteogenic differentiation assessment underlined the beneficial effect of the nanotubes with an intertube spacing of 80 nm [9]. Moreover, the recently established field of osteoimmunology points out that the in vivo osteogenic process is not simply accomplished by the bone-derived cells alone, but through a close collaboration between the skeletal and the immune systems [40]. Therefore, we can now state that the success of the biomaterial's integration depends heavily on the inflammatory-driven process located at and adjacent to the implant's surface [41]. The introduction of an implant into the host's organism is always associated with a surgical injury which on its own will induce a classical pathophysiological acute inflammatory response. Furthermore, depending on the implant's characteristics such as shape, size, surface chemistry and morphology, the biomaterial will be recognised by the host's immune system as a foreign body, therefore resulting in a foreign body reaction (FBR) - a chronic inflammatory state which will hinder the success of the osseointegration process and the implant itself [40]. In this context, in a follow-up in vitro study, our team investigated the effect of TNT interspacing on the inflammatory activity of RAW 264.7 macrophages and the obtained data demonstrated that an 80 nm intertube spacing was capable of reducing the inflammatory activity of macrophages through the modulation of their polarization state towards an anti-inflammatory profile. Overall, the results of this study proved that intertube spacing can represent a passive strategy for macrophage modulation to obtain an inflammatory activity directed towards bone regeneration and osseointegration rather than bone resorption and implant failure [22]. Altogether, these two previous in vitro studies brought forward a new surface feature worthy of a more in-depth investigation, the reason why in the current study the in vivo effect of lateral spacing on the cell-surface interactions and osseointegration was evaluated. The obtained results corroborate previous in vitro findings, suggesting that the optimal intertube spacing for accelerated new bone formation is ≈ 90 nm. The favourable new bone formation could be attributed to the special nanostructure of the implant's surface which combines the positive effect of nanoscale features with an optimal lateral spacing for the regulation of the molecular and cellular activities, which in turn, through various direct and indirect mechanisms, will modulate the osseointegration process [42-44].

5. Conclusions

In the present study, two types of Ti-based implants, namely nanotubes with the typical close-packed (TNTs) or spaced (spTNTs) nanotopography, were obtained with similar morphology on flat Ti (typically used for in vitro tests) and on Ti pins (to be used in in vivo test). The two morphologies show similar chemical composition and mechanical strength (hardness, elastic modulus – at a displacement where only parameters for the nanotube layers are observed). However, as expected due to the spaced morphology, the spTNTs show a higher average roughness in AFM, which is due to the penetration of the AFM tip in between the nanotubes. The layers were evaluated regarding their ability to promote new bone formation and improve the osseointegration process at the implantation site. The histological examination revealed that the nanotubular surfaces did not induce any alterations in the bone marrow's structure and were capable of stimulating the number of osteoblasts and osteoprogenitor cells found at the endosteum level. Moreover, between the two nanotubular surfaces, it was observed that the spTNTs pins were capable of promoting new bone tissue formation to a greater extent than the TNTs surface, with a difference in the average thickness of the newly formed bone tissue of approximately 14.11 μm after 30 days of implantation.

Considering the aspects explored in the current study, it is important to mention that the osseointegration of any implantable medical device represents a very complex process and that the

impact of nanotube spacing, although promising, should be investigated in further detail in its different stages. Moreover, the underlying mechanisms through which these nanotubular surfaces can mediate bone regeneration and bone ingrowth are still unclear, therefore additional studies are necessary in order to fully elucidate the intrinsic molecular mechanisms of these processes.

Author Contributions: Conceptualization, O.Z., A.M., P.S., A.C.; Methodology, A.M.N., I.I., M.G.N.,N.T., O.Z., A.M.; Software, A.M.N, N.T., M.K.; Validation, A.M.N., I.I.; M.G.N., O.Z.; A.M., A.C.; Formal analysis, I.I.; M.G.N., A.M.; Investigation, I.I., M.G.N., N.T., M.K., O.Z., A.M.; Resources, P.S., A.C., Data curation, A.M.N., A.M., A.C.; Writing—original draft preparation, A.M.N., M.G.N., N.T.; O.Z.; A.M.; Writing—review and editing, I.I., A.M., P.S., A.C.; Visualization, A.M.N., I.I., M.G.N., A.M., P.S., A.C.; Supervision, A.C.; Project administration, A.C.; Funding acquisition, A.C.

Funding: This research was funded by the Romanian Ministry of National Education, CNCS-UEFISCDI (Grant PCE 55: Spaced titania nanotubes as platforms for drug delivery and bone regeneration).

Institutional Review Board Statement: The animal study protocol was approved by the Bioethics Committee of the University of Agronomic Sciences and Veterinary Medicine of Bucharest (Approval code No. 07/28.06.2016).
Data Availability Statement: Data sharing is not applicable to this article as no new data were created or analysed in this study.

Conflicts of Interest: The authors declare no conflict of interest.

References

1. Tao, B.; Lan, H.; Zhou, X.; Lin, C.; Qin, X.; Wu, M.; Zhang, Y.; Chen, S.; Guo, A.; Li, K.; Chen, L.; Jiao, Y.; Yi, W. Regulation of TiO2 nanotubes on titanium implants to orchestrate osteo/angio-genesis and osteo-immunomodulation for boosted osseointegration. *Mater. Des.* **2023**, *233*, 112268, doi: 10.1016/j.matdes.2023.112268.
2. Messias, A.; Nicolau, P.; Guerra, F. Titanium dental implants with different collar design and surface modifications: a systemic review on survival rates and marginal bone levels. *Clin. Oral Implan. Res.* **2019**, *30*, 20-48, doi: 10.1111/clr.13389.
3. Ma, A.; Shang, H.; Song, Y.; Chen, B.; You, Y.; Han, W.; Zhang, X.; Zhang, W.; Li, Y.; Li, C Icariin-Functionalised Coating on TiO2 Nanotubes Surface to Improve Osteoblast activity in Vitro and Osteogenesis Ability in Vivo. *Coatings* **2019**, *9*, 327, doi: 10.3390/coatings9050327.
4. Liu, X, Chu, P.K.; Ding, C. Surface modification of titanium, titanium alloys, and related materials for biomedical applications. *Mater. Sci. Eng. R Rep.* **2004**, *47*, 49-121, doi: 10.1016/j.mser.2004.11.001.
5. Khaw, J.S.; Bowen, C.R.; Cartmell, S.H. Effect of TiO2 Nanotube Pore Diameter on human Mesenchymal Stem Cells and Human Osteoblasts. *Nanomaterials* **2020**, *10*, 2117, doi: 10.3390/nano10112117.
6. Lin, L.; Wang, H.; Ni, M.; Rui, Y.; Cheng, T.; Cheng, C.; Pan, X.; Li, G.; Lin, C. Enhanced osteointegration of medical titanium implant with surface modifications in micro/nanostructures. *J. Orthop. Transl*. **2014**, *2*, 35-42, doi:10.1016/jot.2013.08.001.
7. Izmir, M.; Ercan, B. Anodization of titanium alloys for orthopedic applications. *Front. Chem. Sci. Eng*. **2019**, *13*, 28-45, doi: 10.1007/s11705-018-1759-y.
8. Roy, P.; Berger, S.; Schmuki, P. TiO2 nanotubes: Synthesis and applications. *Angew. Chem. Int. Ed. Engl.* **2011**, *50*, 2904-2939, doi: 10.1002/anie.201001374.
9. Necula, M.G.; Mazare, A.; Ion, R.N.; Ozkan, S.; Park, J.; Schmuki, P.; Cimpean, A. Lateral Spacing of TiO2 Nanotubes Modulates Osteoblast Behavior. *Materials* **2019**, *12*, 2956, doi: 10.3390/ma12182956.
10. Bjursten, L.M.; Rasmusson, L.; Oh, S.; Smith, G.C.; Brammer, K.S.; Jin, S. Titanium dioxide nanotubes enhance bone bonding in vivo. J. Biomed. Mater. Res. A 2010, 1218-1224, doi: 10.1002/jgm.a.32463.
11. von Wilmowsky, C.; Bauer, S.; Lutz, R.; Meisel, M.; Neukam, F.W.; Toyoshima, T.; Schmuki, P.; Nkenke, E.; Schlegel, K.A. In Vivo Evaluation of Anodic TiO2 Nanotubes: An experimental Study in the Pig. J. Biomed. Mater. Res. Part B: Appl. Biomater. 2009, 89, 165-171, doi: 10.1002/jbm.b.31201.
12. Kang, C.-G.; Park, Y.-B.; Choi, H.; Oh, S.; Lee, K.-W.; Choi, S.-H.; Shim, J.-S. Osseointegration of Implants Surface-treated with Various Diameters of TiO2 Nanotubes in Rabbit. Journal of Nanomaterials 2015, 1-11, doi: 10.1155/2015/634650.
13. Wang, N.; Li, H.; Lu, W.; Li, J.; Wang, J.; Zhang, Z.; Liu, Y. Effects of TiO2 nanotubes with different diameters on gene expression and osseointegration of implants in minipigs. Biomaterials 2011, 32, 6900-6911, doi: 10.1016/j.biomaterials.2011.06.023
14. Jang, I.; Shim, S.-C.; Choi, D.-S.; Cha, B.-K.; Lee, J.-K.; Choe, B.-H.; Choi, W.-Y. Effect of TiO2 nanotubes arrays on osseointegration of orthodontic miniscrew. Biomed. Microdevices 2015, 17, 76, doi: 10.1007/s10544-015-9986-1.

15. Park, J.; Bauer, S.; Von Der Mark, K.; Schmuki, P.; Nanosized and Vitality: TiO2 Nanotube Diameter Directs Cell Fate. Nano Lett. 2007, *7*, 1687-1691;
16. Park, J.; Bauer, S.; Schlegel, K.A.; Neukam, F.M. Von Der Mark, K.; Schmuki, P. TiO2 nanotube surfaces: a 15nm-an optimal length scale of surface topography for cell adhesion and differentiation. *Small* **2009**, *5*, 666-671, doi: 10.1002/smll.200801476.
17. Xu, L.; Yu, Q.; Jiang, X.Q.; Zhan, F.Q.; Yu, W.; Jiang, X.; Zhang, F. The effect of anatase TiO2 nanotube layers on MC3T3-E1 preosteoblasts adhesion, proliferation and differentiation. *J. Biomed. Mater. Res. Part A* **2010**, *94*, 1012-1022, doi: 10.1002/jbm.a.32687.
18. Che, C.; Wang, J.; Guo. W. Effect of TiO2 Nanotubes on Biological Activity of Osteoblasts and Focal Adhesion Kinase/Osteopontin Level. *J. Biomed. Technol.* **2024**, *20*, 793-799, doi: 10.1166/jbn.2024.3877.
19. Brammer, K.S.; Oh, S.; Cobb, C.J.; Bjursten, L.M.; van der Heyde, H.; Jin, S. Improved bone-forming functionality of diameter-controlled TiO2 nanotube surface. *Acta Biomater.* **2009**, *5*, 3215-3223, doi:10.1016/j.actabio.2009.05.008.
20. Yi, Y.; Park, Y.; Choi, H.; Lee, K.; Kim, S.; Kim, K.; Oh, S.; Shim, J. The Evaluation of Ossoeintegration of Dental Implant Surface with Different Size of TiO2 Nanotube in Rats. *Journal of Nanomaterials* **2015**, *2015*, 11, doi: 10.1155/2015/581713.
21. von Wilmowsky, C.; Bauer, S.; Roedl, S.; Neukam, F.W.; Schmuki, P.; Schlegel, K.A. The diameter of anodic TiO2 nanotubes affects bone formation and correlates with the bone morphogenic protein-2 expression in vivo. *Clin, Oral Implants Res*. **2011**, *23*, 359-366, doi: 10.1111/j.1600-0501.2010.02139x.
22. Necula, M.G.; Mazare, A.; Negrescu, A.M.; Mitran, V.; Ozkan, S.; Trusca, R.; Park, J.; Schmuki, P.; Cimpean, A. Macrophage-like Cells Are Responsive to Titania Nanotube Intertube Spacing – An In Vitro Study. *Int. J. Mol. Sci.* **2022**, *23*, 3558, doi: 10.3390/ijms23073558.
23. Özkan, S.; Nguyen, N.T.; Mazare, A.; Schmuki, P. Controlled spacing of self-organized anodic TiO2 nanotubes. *Electrochem. Commun*. **2016**, *69*, 76–79, doi: 10.1016/j.elecom.2016.06.004
24. Ozkan, S.; Nguyen, N.T.; Mazare, A.; Hahn, R.; Cerri, I.; Schmuki, P. Fast growth of TiO2 nanotube arrays with controlled tube spacing based on a self-ordering process at two different scales. *Electrochem. Commun*. **2017**, *77*, 98–102, doi: 10.1016/j.elecom.2017.03.007.
25. Nguyen, N.T.; Ozkan, S.; Hwang, I.; Mazare, A.; Schmuki, P. TiO2 nanotubes with laterally spaced ordering enable optimized hierarchical structures with significantly enhanced photocatalytic H2 generation. Nanoscale **2016**, *8*, 16868–16873, doi: 10.1039/C6NR06329B.
26. Ozkan, S.; Cha, G.; Mazare, A.; Schmuki, P. TiO2 nanotubes with different spacing, Fe2O3 decoration and their evaluation for Li-ion battery application. *Nanotechnology* **2018**, *29*, 195402, doi: 10.1088/1361-6528/aab062.
27. Ozkan, S.; Valle, F.; Mazare, A.; Hwang, I.; Taccardi, N.; Zazpe, R.; Macak, J.M.; Cerri, I.; Schmuki, P. Optimized Polymer Electrolyte Membrane Fuel Cell Electrode Using TiO2 Nanotube Arrays with Well-Defined Spacing. *ACS Appl. Nano Mater*. **2020**, *3*, 4157–4170, doi: 10.1012/acsanm.0c00325.
28. Ozkan, S.; Mazare, A.; Schmuki, P. Critical parameters and factors in the formation of spaced TiO2 nanotubes by self-organizing anodization. *Electrochim. Acta* **2018**, *268*, 435–447, doi: 10.1016/j.electacta.2018.02.120.
29. Xu, Y.N.; Liu, M.N.; Wang, M.C.; Oloyede, A.; Bell, J.M.; Yan, C. Nnaoindentation study of the mechanical behavior of the TiO2 nanotube arrays. *J. Appl. Phys*. **2015**, *118*, 145301.
30. Cruz, M.B.; Silva, N.; Marques, J.F.; Mata, A.; Silva, F.S.; Carames, J. Biomimetic Implant Surfaces and Their Role in Biological Integration – A Concise Review. *Biomimetics* **2022**, *7*, 74, doi: 10.3390/biomimetics7020074
31. Agarwal, R.; Garcia, A.J. Biomaterial strategies for engineering implants for enhanced osseointegration and bone repair. *Adv. Drug Deliv Rev*. **2015**, *94*, 53-62, doi: 10.1016/j.addr.2015.03.013.
32. Alves-Rezende, M.C.; Capalbo, L.C.; De Oliveira Limirio, J.P.J.; Capalbo, B.C.; Limirio, P.H.J.O.; Rosa, J.L. The role of TiO2 nanotube surface on osseointegration of titanium implants: Biomechanical and histological study in rats. *Micros. Res. Tech*. **2020**, 1-7.
33. Wang, C.; Gao, S.; Lu, R.; Wang, X.; Chen, S. In Vitro and In Vivo Studies of Hydrogenated Titanium Dioxide Nanotubes with Superhydrophilic Surfaces during Early Osseointegration. *Cells* **2022**, *11*, 3417.
34. Li, J.; Zheng, Y.; Yu, Z.; Kankala, R.K.; Lin, Q.; Shi, J.; Chen, C.; Luo, K.; Chen, A.; Zhong, Q. Surface-modified titanium and titanium-based alloys for improved osteogenesis: A critical review. *Heliyon* **2024**, *10*, e23779.
35. Zhao, X.; You, L.; Wang, T.; Zhang, X.; Li, Z.; Ding, L.; Li, J.; Xiao, C.; Han, F.; Li, B. Enhanced Ossoeintegration of Titanium Implants by Surface Modification with Silicon-doped Titania Nanotubes. *Int. J. Nanomed*. **2020**, *15*, 8583-8594.
36. Yao, L.; Al-Bishari, A.M.; Shen, J.; Wang, Z.; Liu, T.; Sheng, L.; Wu, G.; Lu, L.; Xu, L.; Liu, J. Ossoeintegration and anti-infection of dental implant under osteoporotic conditions promoted by gallium oxide nano-layer coated titanium dioxide nanotube arrays. *Ceramics International* **2023**, *49*, 22961-22969.

37. Moon, K.-S.; Bae, J.-M.; Park, Y.-B.; Choi, E.-J.; Oh, S.-H. Photobiomodulation-Based Synergic Effects of Pt-Coated TiO2 Nanotubes and 850nm Near-Infrared Irradiation on the Ossoeintegration Enhancement: In Vitro and In Vivo Evaluation. *Nanomaterials* **2023**, *13*, 1377.
38. Li, Y.; Tang, L.; Shen, M.; Wang, Z.; Huang, X. A comparative study of Sr-loaded nano-textured Ti and TiO2 nanotube implants on osseointegration immediately after tooth extraction in Beagle dogs. *Front. Mater*. **2023**, *10*, 1213163.
39. Hamlekhan, A.; Takoudis, C.; Sukotjo, C.; Mathew, M.T.; Virdi, A.; Shahbazian-Yassar, R.; Shokuhfar, T. Recent progress toward surface modification of bone/Dental implants with titanium and zirconia dioxide nanotubes fabrication of TiO2 nanotubes. *J. Nanotechnol. Smart Mater*. **2014**, *1*, 301-314.
40. Miron, R.J.; Bohner, M.; Zhang, Y.; Bosshardth, D.D. Ostoeinduction and osteoimmunology: Emerging concepts. Periodontology 2000 2024, 94, 9-26, doi: 10.1111/prd.12519.
41. Bai, L.; Du, Z.; Du, J.; Yao, W.; Zhang, J.; Weng, Z.; Liu, S.; Zhao, Y.; Liu, Y.; Zhang, X.; Huang, X.; Yao, X.; Crawford, R.; Hang, R.; Huang, D.; Tang, B.; Xiao, Y. A multifaceted coating on titanium dictates osteoimmunomodulation and osteo/angio-genesis towards ameliorative osseointegration. Biomaterials 2018, 162, 154-169, doi: 10.1016/j.biomaterials.2018.02.010.
42. Mendonca, G.; Mendonca, D.B.; Simoes, L.G.; Araujo, A.L.; Leite, E.R.; Duarte, W.R.; Aragao, F.J.L.; Cooper, L.F. The effects of implant surface nanoscale features of osteoblast specific gene expression. *Biomaterials* **2009**, *30*, 4053, 4062, doi: 10.1016/j.biomaterials.2009.04.010.
43. Shekaran, A.; Garcia, A.J. Nanoscale engineering of extracellular matrix-mimetic bioadhesive surfaces and implants for tissue engineering. *Biochem. Biophys. Acta*. **2011**, *1810*, 350-360, doi: 10.1016/j.bbagen.2010.04.006.
44. Wang, N.; Li, H.; Lu, W.; Li, J.; Wang, J.; Zhang, Z.; Liu, Y. Effects of TiO2 nanotubes with different diameters on gene expression and osseointegration of implants in minipigs. *Biomtaterials* **2011**, *32*, 6900-6911, doi10.1016/j.biomaterials.2011.06.02.